Supplementary Materials

for

Haploinsufficiency of the 22q11.2-microdeletion gene *Mrpl40* disrupts short-term synaptic plasticity and working memory through dysregulation of mitochondrial calcium

Prakash Devaraju[1], Jing Yu[1], Donnie Eddins[1], Marcia M. Mellado-Lagarde[1], Laurie R. Earls[1,3], Joby J. Westmoreland[1,3], Giovanni Quarato[2], Douglas R. Green[2] and Stanislav S. Zakharenko[1,*]

[1]Department of Developmental Neurobiology, [2]Department of Immunology, St. Jude Children's Research Hospital, Memphis, TN 38105, USA. [3]Present address: Department of Cell and Molecular Biology, Tulane University, New Orleans, LA, 70118, USA

Contact information:

Stanislav S. Zakharenko M.D., Ph.D.
Department of Developmental Neurobiology
Mail Stop 323
St. Jude Children's Research Hospital
Memphis, TN 38105, USA
[*]E-mail: stanislav.zakharenko@stjude.org

Supplementary Figures

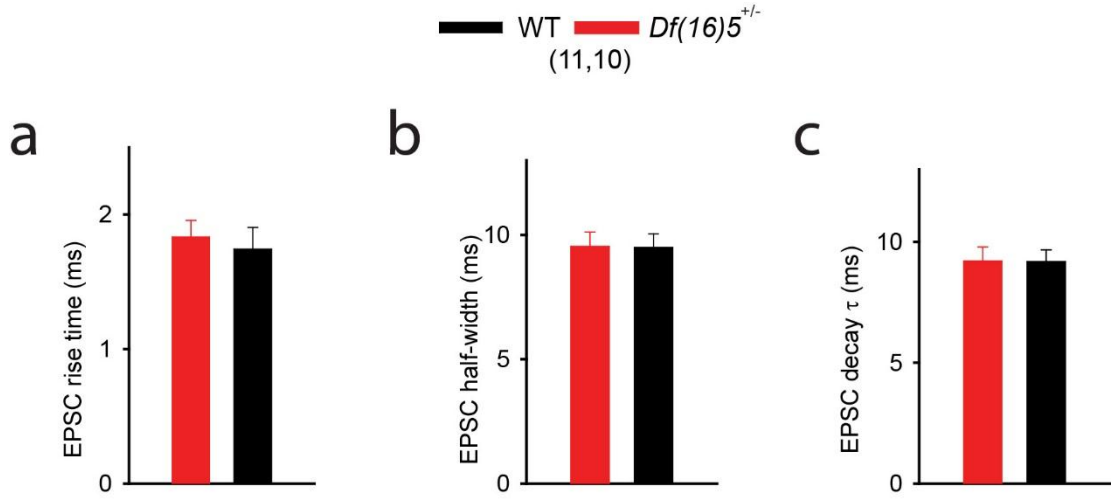

Supplementary Figure 1. Normal EPSC kinetics in *Df(16)5*$^{+/-}$ mice. The $EPSC_{20\%-80\%}$ rise time (**a**), half-width (**b**), and decay constant (**c**) were calculated in WT and *Df(16)5*$^{+/-}$ mice. Numbers of neurons tested are shown in parenthesis.

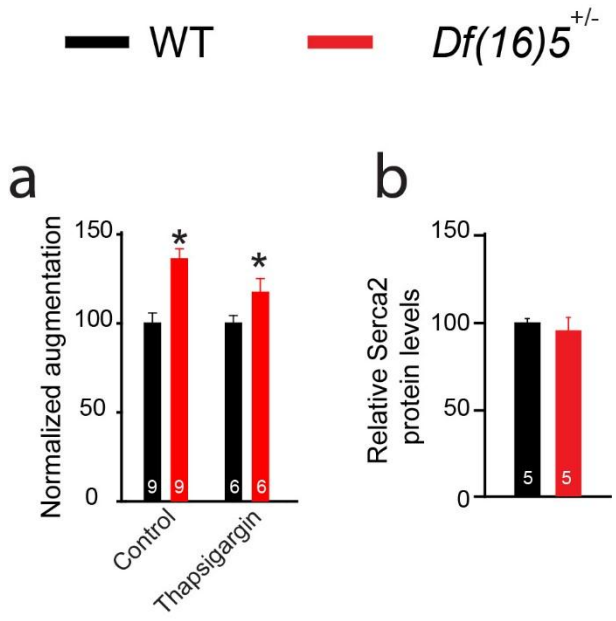

Supplementary Figure 2. SERCA2 is not involved in STP abnormalities in *Df(16)5*$^{+/-}$ mice. (a) Mean augmentation in *Df(16)5*$^{+/-}$ mice and their respective WT littermates (normalized to augmentation in respective WT mice), in the absence or presence of thapsigargin. (b) Western blot analysis of Serca2 showed that the protein's level in the hippocampi of *Df(16)5*$^{+/-}$ mice was comparable to that of WT littermates. Numbers of neurons or mice are shown inside columns. Data are represented as mean ± SEM. **P* <0.05.

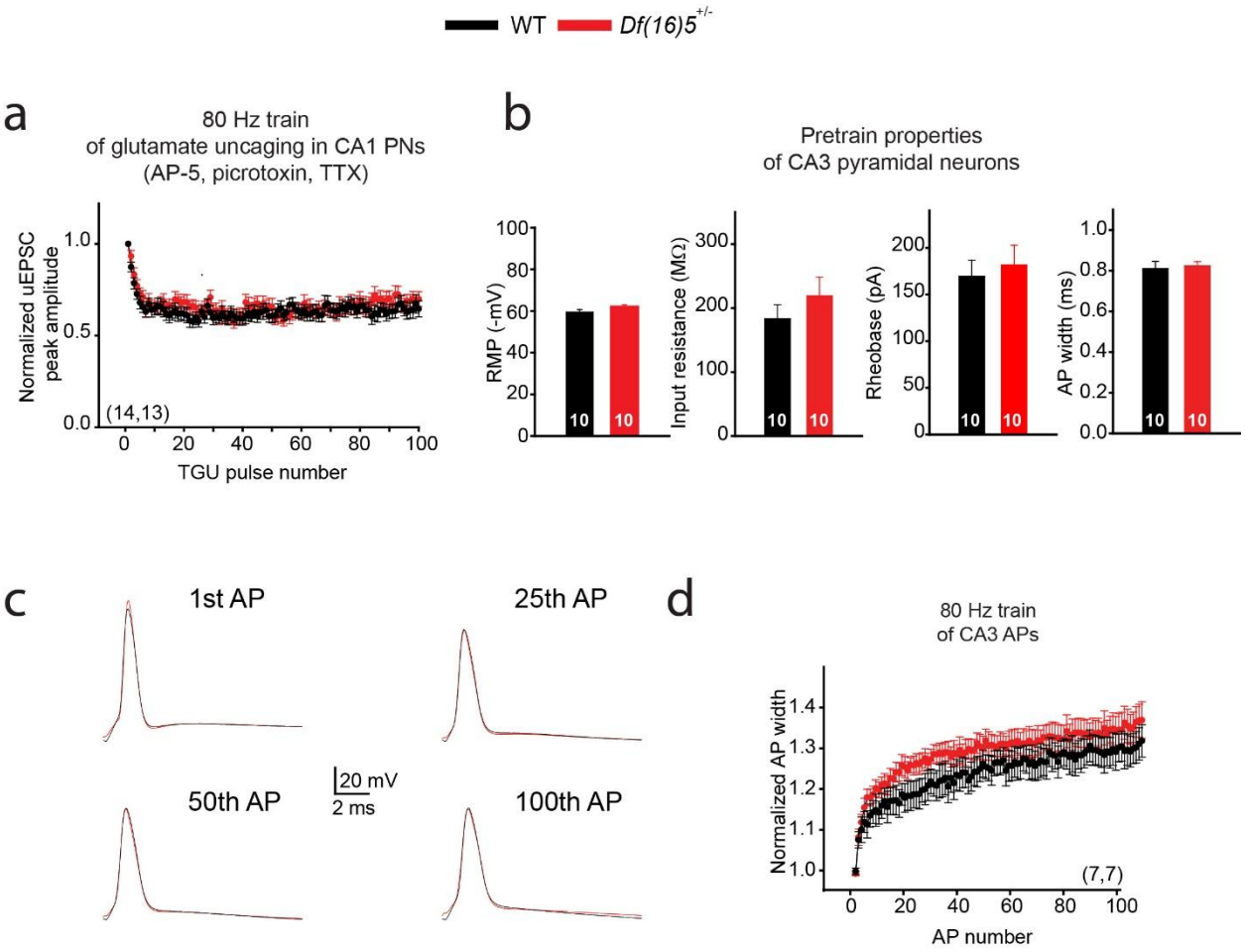

Supplementary Figure 3. Normal postsynaptic function and CA3 (presynaptic) action potential generation in *Df(16)5*$^{+/-}$ mice. (**a**) Two-photon glutamate uncaging (TGU) at a single dendritic spine evoked EPSCs (uEPSCs) in CA1 neurons. Normalized uEPSC is plotted as a function of uncaging pulses in CA1 hippocampal neurons of WT and *Df(16)5*$^{+/-}$ mice during the 80-Hz train of TGU. D-2-amino-5-phosphonovalerate (D-AP5, 50 µM), picrotoxin (100 µM), and tetrodotoxin (TTX, 1 µM) were added to the extracellular solution to prevent long-term synaptic plasticity, polysynaptic inhibitory activity, and the generation of action potentials (APs), respectively. (**b**) Normal excitability of presynaptic CA3 neurons. Average resting membrane potential (RMP) (left), input resistance (left middle), rheobase (right middle), and AP width (right) were recorded in CA3 neurons of WT and *Df(16)5*$^{+/-}$ mice prior to the 80-Hz train. (**c**, **d**) Representative traces of the 1st, 25th, 50th, and 100th APs (**c**) and normalized AP width (**d**) during the 80-Hz train of depolarization pulses in CA3 neurons of WT and *Df(16)5*$^{+/-}$ mutants. Numbers of neurons are shown in parentheses or inside the columns.

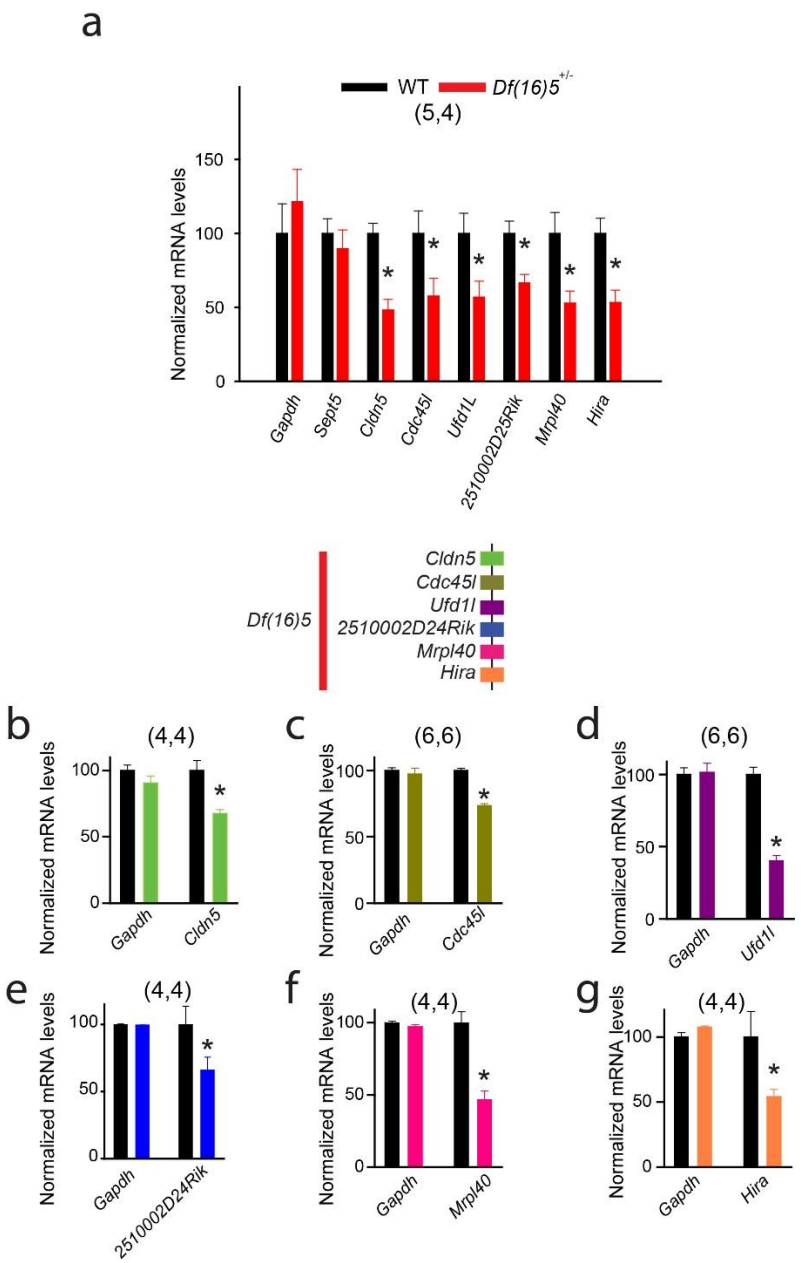

Supplementary Figure 4. Transcript levels in the hippocampus and cortex of *Df(16)5*$^{+/-}$ mice and mice with hemizygous deletions of individual genes within the *Df(16)5* genomic region. (**a**) Normalized mRNA levels of the following *Df(16)5* genes: *Cldn5*, *Cdc45l, Ufd1l, 2510002D25Rik, Mrpl40,* and *Hira* in *Df(16)5*$^{+/-}$ mice. *Gapdh,* a housekeeping gene, and *Sept5*, a 22q11DS gene outside the *Df(16)5* microdeletion, are used as negative controls. (**b**-**g**) Normalized mRNA levels of *Gapdh* and *Cldn5* (**b**), *Cdc45l* (**c**), *Ufd1l* (**d**), *2510002D25Rik* (**e**), *Mrpl40* (**f**), and *Hira* (**g**) genes in WT mice and respective *Cldn5*$^{+/-}$ (**b**), *Cdc45l*$^{+/-}$ (**c**), *Ufd1l*$^{+/-}$ (**d**), *2510002D25Rik*$^{+/-}$ (**e**), *Mrpl40*$^{+/-}$ (**f**), and *Hira*$^{+/-}$ (**g**) littermates. Numbers of mice are shown in parentheses. **P* <0.05.

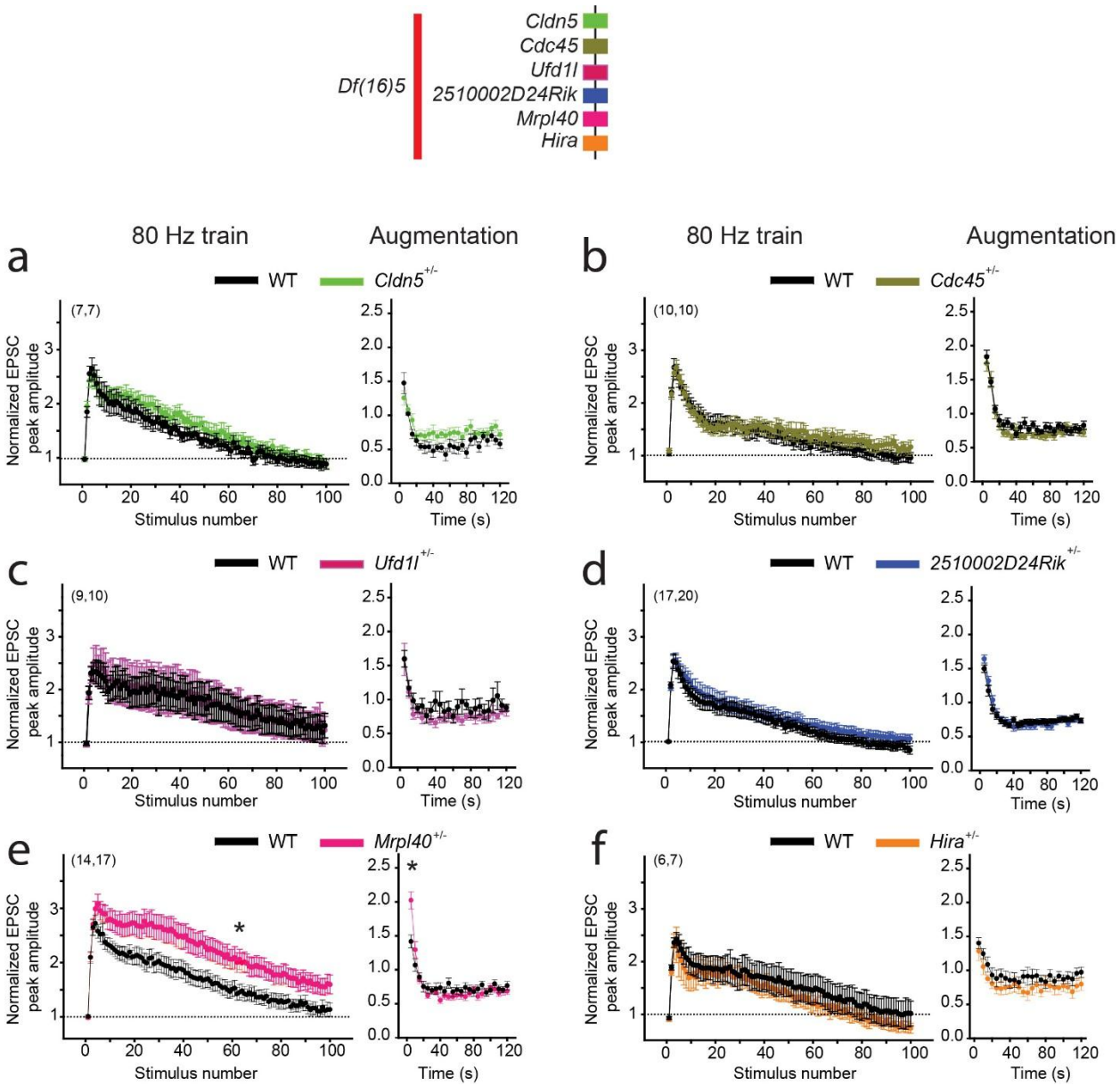

Supplementary Figure 5. Hemizygous *Mrpl40* deletion causes abnormal STP and augmentation. Mean STP of EPSCs induced by the 80-Hz train of synaptic stimulation of Schaffer collaterals and augmentation measured 5 to 120 s following the 80-Hz train in *Cldn5*$^{+/-}$ (**a**), *Cdc45*$^{+/-}$ (**b**), *Ufd1l*$^{+/-}$ (**c**), *2510002D24Rik*$^{+/-}$ (**d**), *Mrpl40*$^{+/-}$ (**e**), and *Hira*$^{+/-}$ (**f**) mice and their WT littermates. Numbers of neurons are shown in parentheses. Data are represented as mean ± SEM. **P* <0.05.

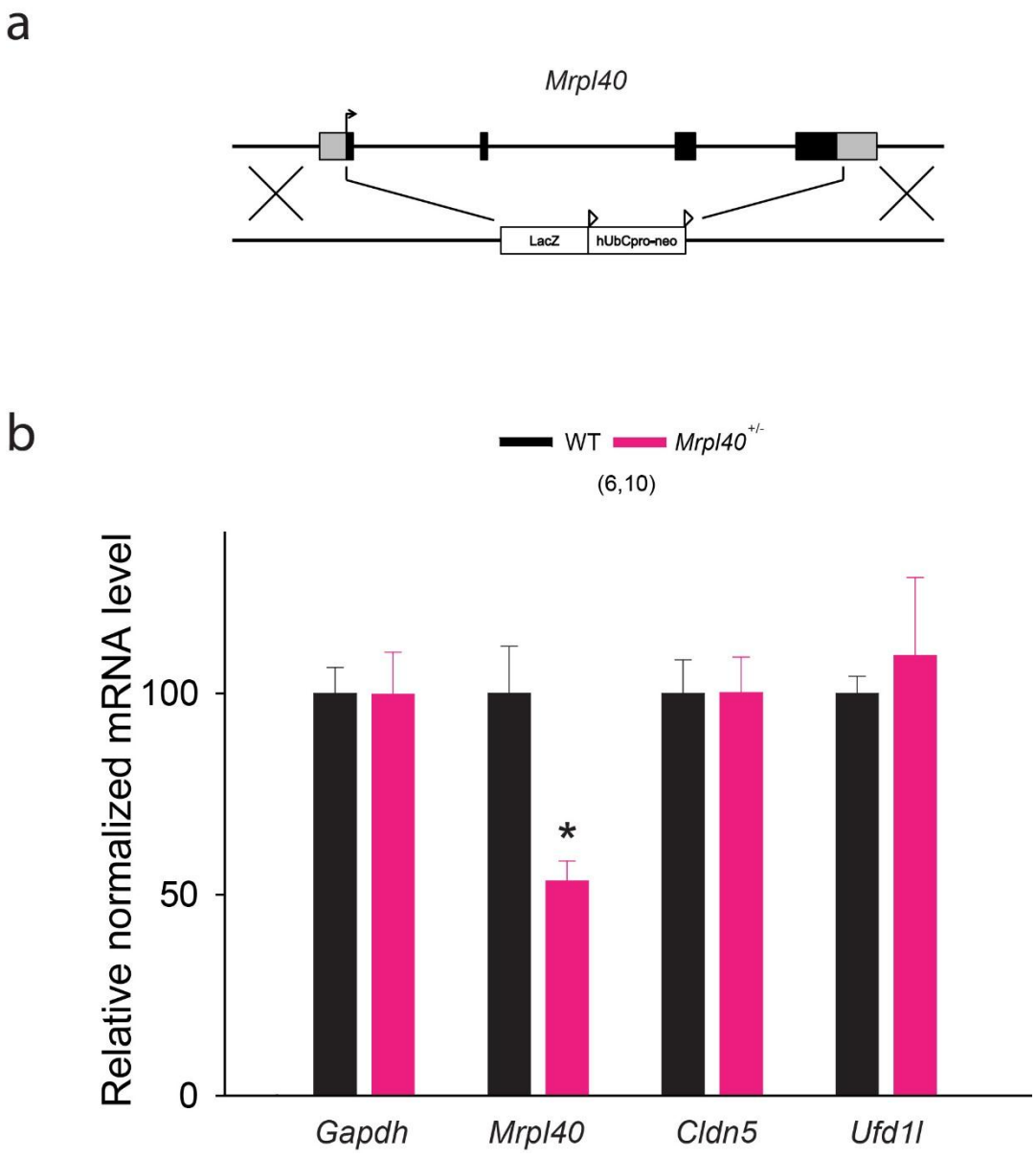

Supplementary Figure 6. *Mrpl40* haploinsufficiency does not affect the expression of other *Df(16)5* genes. (**a**) Diagram of the design used to generate *Mrpl40*$^{+/-}$ mice. (**b**) Normalized mRNA levels of *Gapdh*, *Mrpl40*, *Cldn5*, and *Ufd1l* in WT and *Mrpl40*$^{+/-}$ mice. Numbers of mice are shown in parentheses. **P* <0.05.

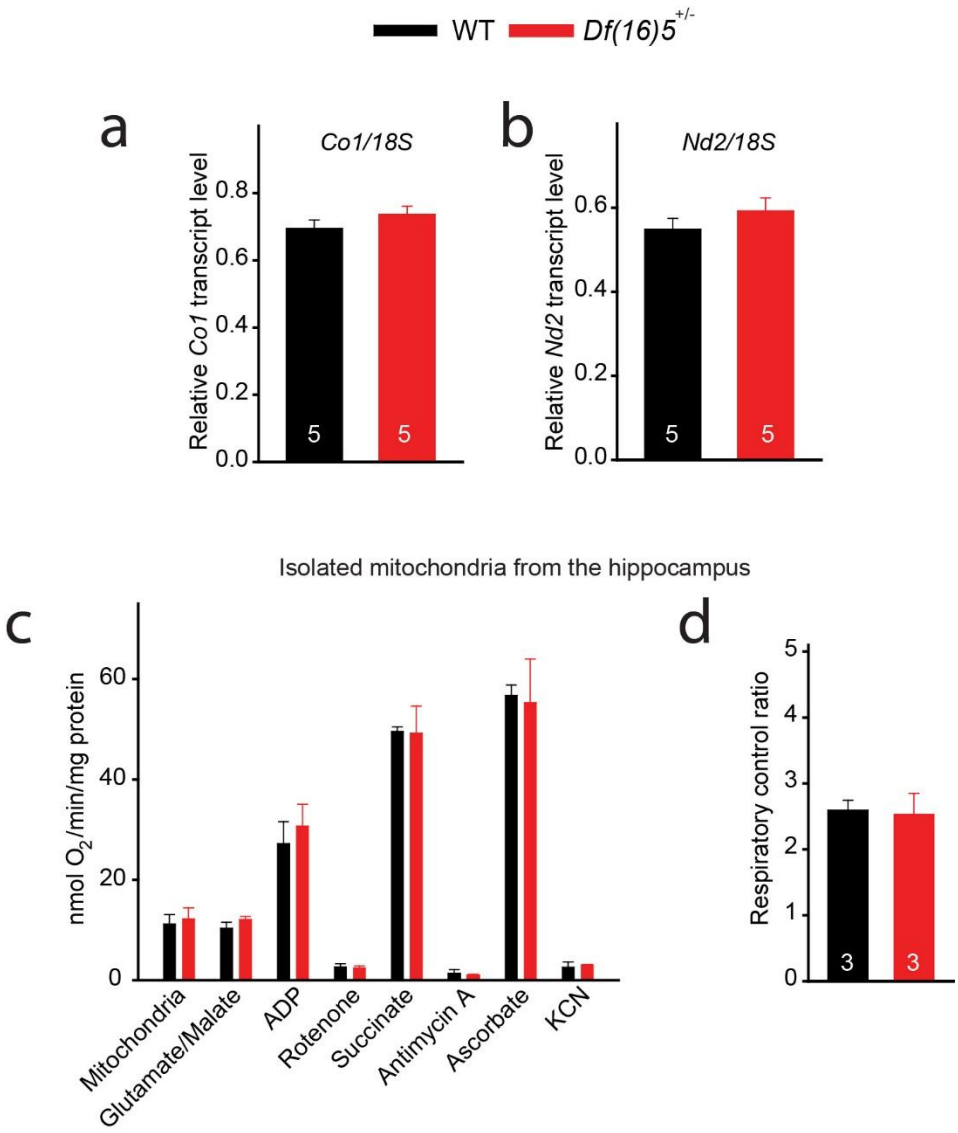

Supplementary Figure 7. Normal levels of mitochondrial mRNAs and oxidative phosphorylation in *Df(16)5*$^{+/-}$ mice. (**a**, **b**) Transcript levels of *Co1*(**a**) and *Nd2* (**b**) were normalized to the nuclear transcript *18S* in the hippocampi of WT and *Df(16)5*$^{+/-}$ mice. (**c**, **d**) Oxidative phosphorylation (**c**) and the respiratory control ratio (**d**) were measured in mitochondria isolated from the hippocampi of WT and *Df(16)5*$^{+/-}$ mice. Numbers of mice are shown inside the columns.

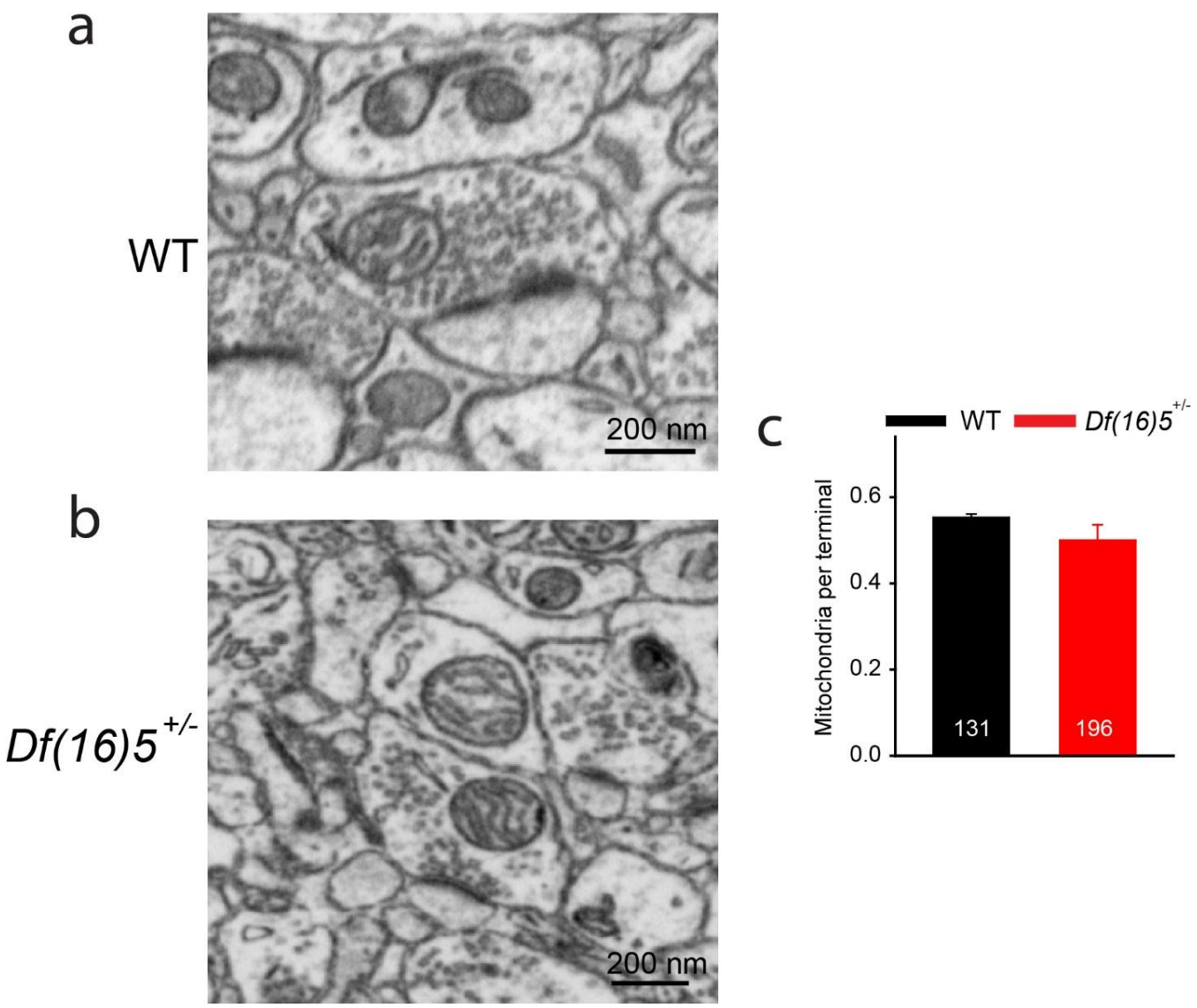

Supplementary Figure 8. The number of mitochondria in presynaptic terminals of *Df(16)5*$^{+/-}$ mice is normal. Representative images of presynaptic terminals with mitochondria and synaptic densities in the same plane cropped from 3D EM stack of hippocampal CA1 area (**a**, **b**) and average numbers of mitochondria in presynaptic terminals (**c**) of WT (2 mice) and *Df(16)5*$^{+/-}$ hippocampi (2 mice). Numbers of presynaptic terminals are shown inside the columns.

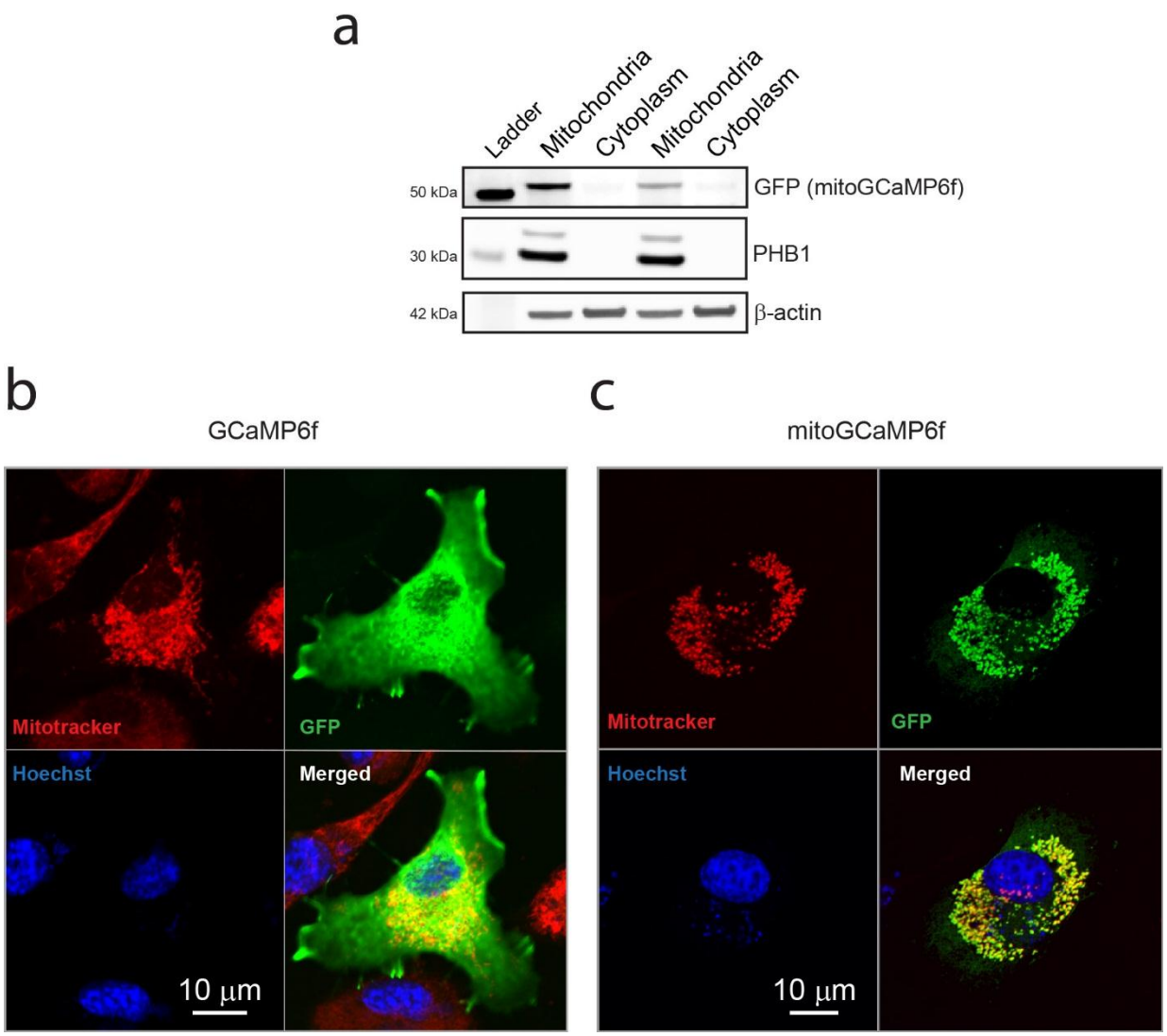

Supplementary Figure 9. GCaMP6 is expressed in cytosol and mitoGCaMP6 is expressed in mitochondria. (**a**) Western blotting for GFP (mitoGCaMP6), mitochondrial protein PHB1, and β-actin in mitochondrial and cytosolic fractions of the hippocampus infected with *AAV-mitoGCaMP6* (2 mice each). (**b**, **c**) Representative fluorescence images of cytosolic GCaMP6 (**b**) and mitoGCaMP6 (**c**) expression in N2a cells transfected with respective plasmids. Mitotracker (red) labels mitochondria; GFP (green) labels cytosol (**b**) or mitochondria (**c**), and Hoechst stain (blue) labels nuclei.

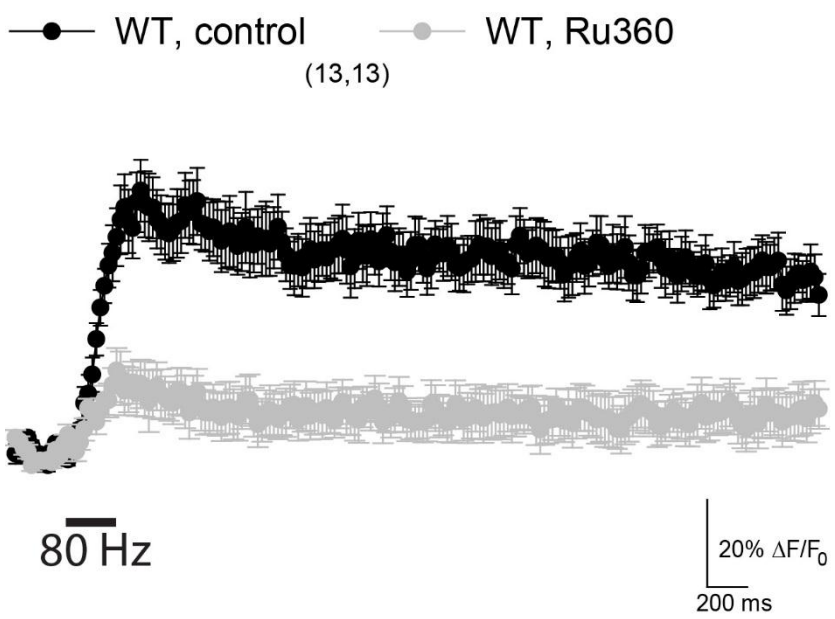

Supplementary Figure 10. Transient mitoGCaMP6 fluorescence is blocked by Ru360, which inhibits the mitochondrial calcium uniporter. Mean mitoGCaMP6 fluorescence as a function of time was measured in the stratum radiatum of WT mice, in response to the 80-Hz synaptic stimulation, in the absence or presence of Ru360 (10 µM). Numbers of boutons are shown in parentheses.

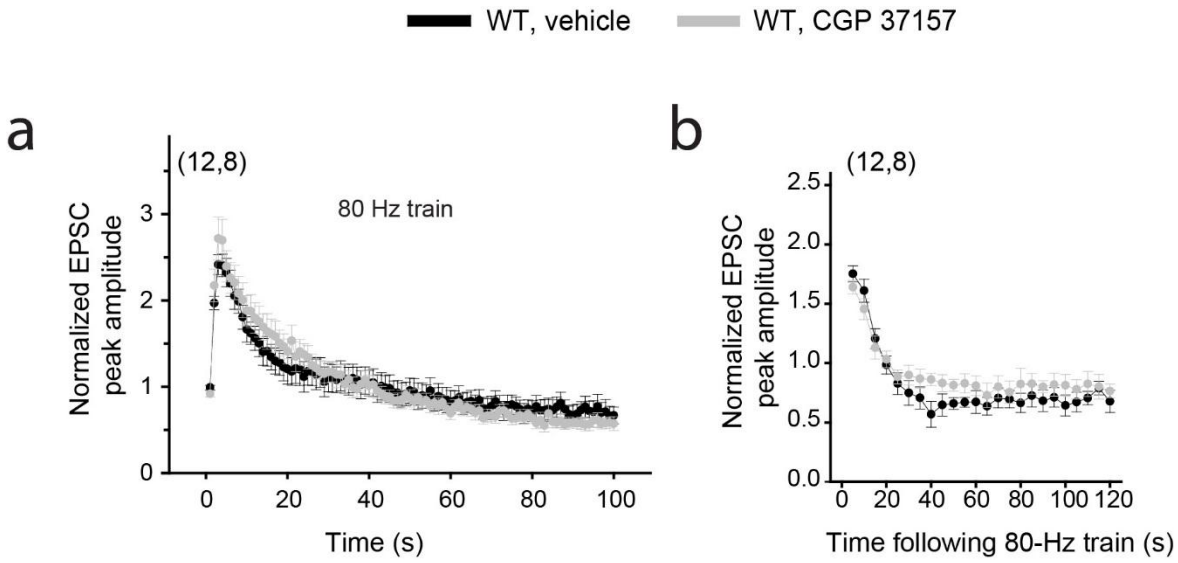

Supplementary Figure 11. STP and augmentation are not affected by the inhibitor of the mitochondrial Na^+–Ca^{2+} exchanger. STP induced by the 80-Hz train of synaptic stimulation (**a**) and augmentation (**b**) at CA3–CA1 synapses of WT mice in the absence or presence of CGP 37157 (5 μM), an inhibitor of the mitochondrial Na^+–Ca^{2+} exchanger. Numbers of neurons tested are shown in parentheses.

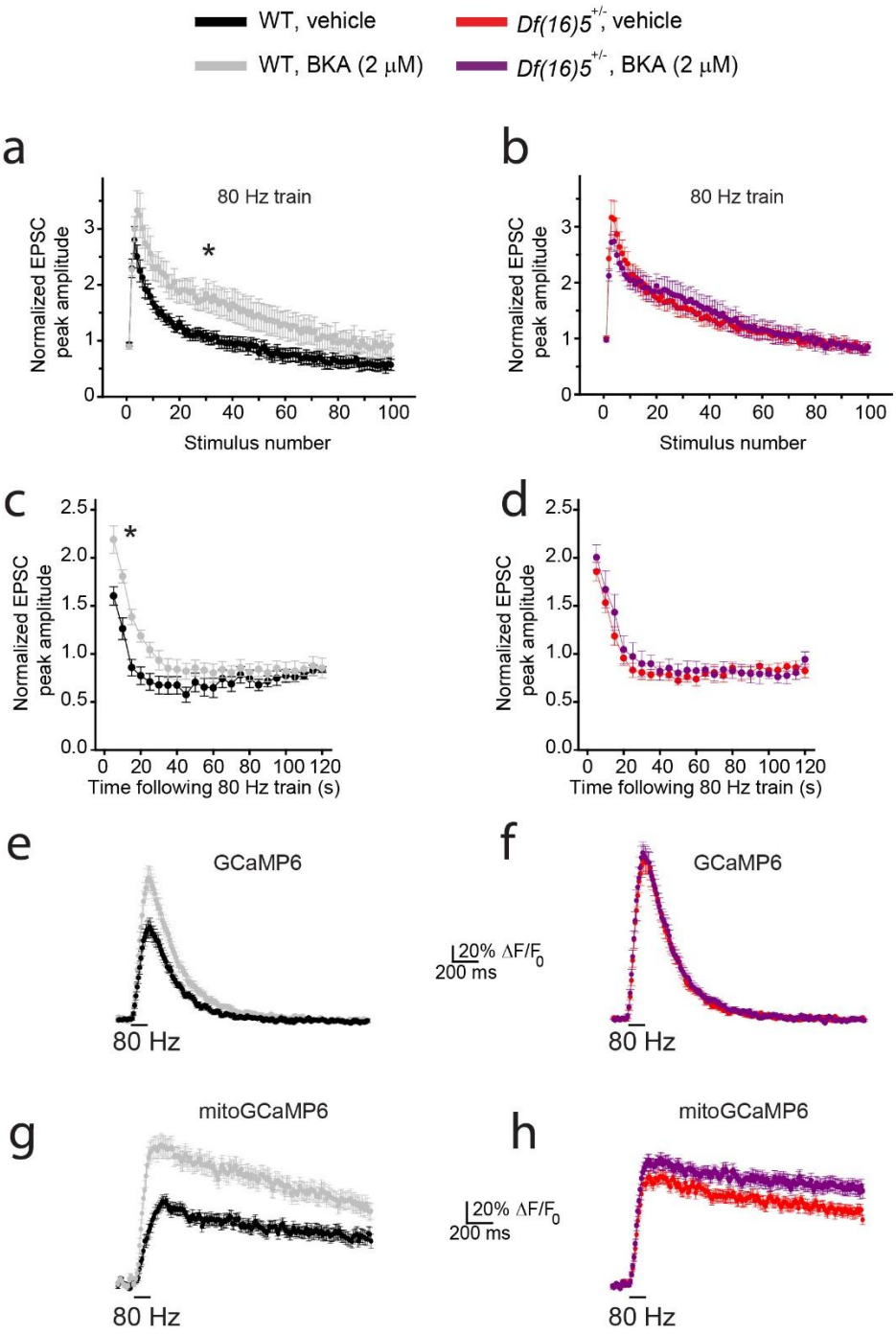

Supplementary Figure 12. The mPTP inhibitor BKA mimics the STP and calcium transient phenotypes of *Df(16)5*$^{+/-}$ mice. (**a-d**) Mean EPSCs during (**a**, **b**) and after (**c**, **d**) the 80-Hz train in WT (**a**, **c**) and *Df(16)5*$^{+/-}$ (**b**, **d**) mice in the absence or presence of BKA. (**e,f**) Average normalized cytosolic GCaMP6 fluorescence intensity as a function of time during the 80-Hz train in WT (**e**) and *Df(16)5*$^{+/-}$ (**f**) mice. (**g, h**) Average normalized mitoGCaMP6 fluorescence intensity as a function of time during the 80-Hz train in WT (**g**) and *Df(16)5*$^{+/-}$ (**h**) mice. **P* <0.05.

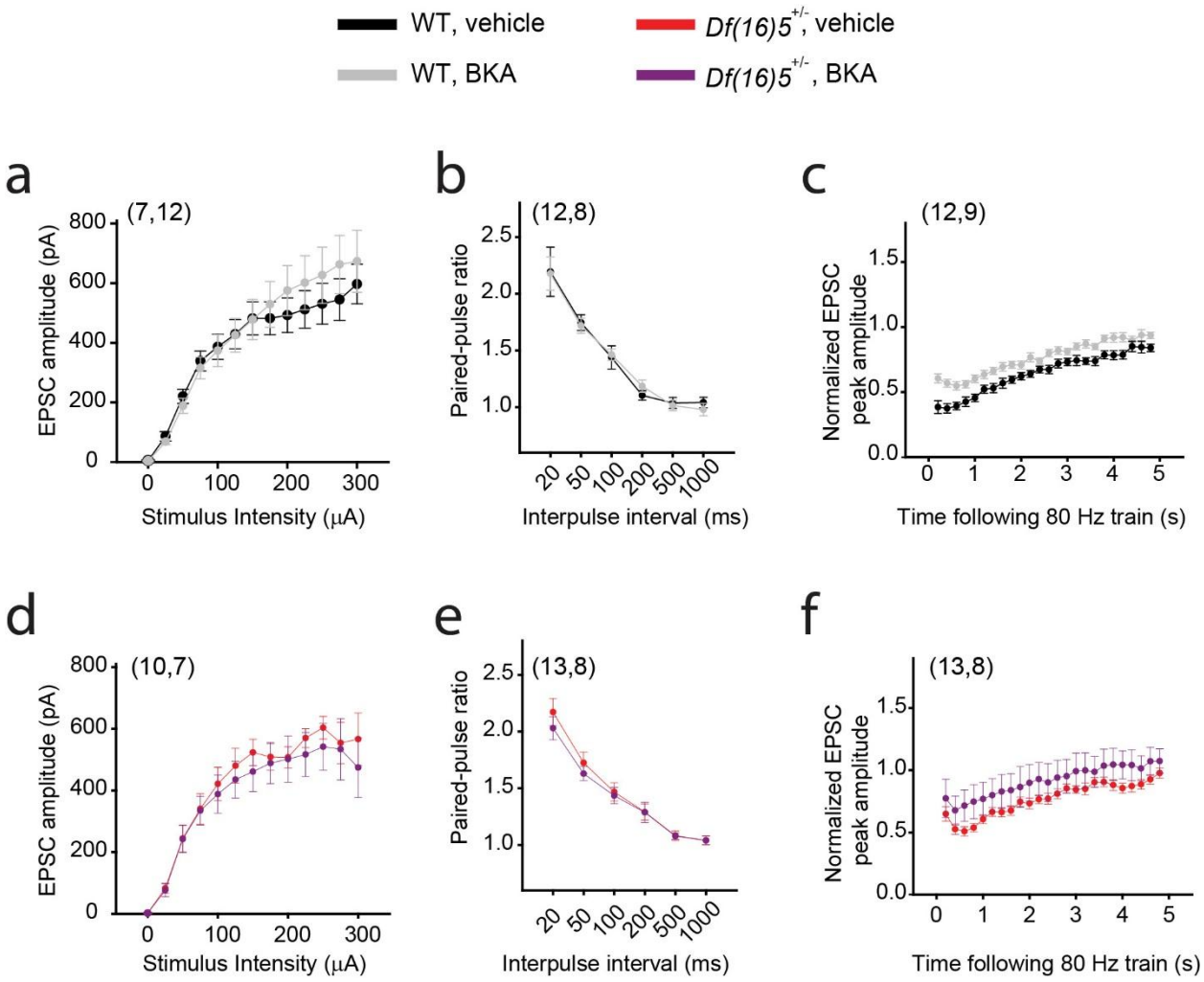

Supplementary Figure 13. The mPTP inhibitor BKA does not affect basal synaptic transmission, synaptic facilitation, or recovery from depression. Mean EPSCs as a function of stimulation intensity (**a**, **d**), paired-pulse ratio of EPSCs as a function of interpulse interval (**b**, **e**), and recovery of EPSCs from depression after the 80-Hz train of synaptic stimulation (**c**, **f**), at CA3–CA1 synapses of WT mice (**a**-**c**) and *Df(16)5*$^{+/-}$ mice (**d**-**f**), in the absence or presence of BKA (2 μM). Numbers of neurons tested are shown in parentheses.

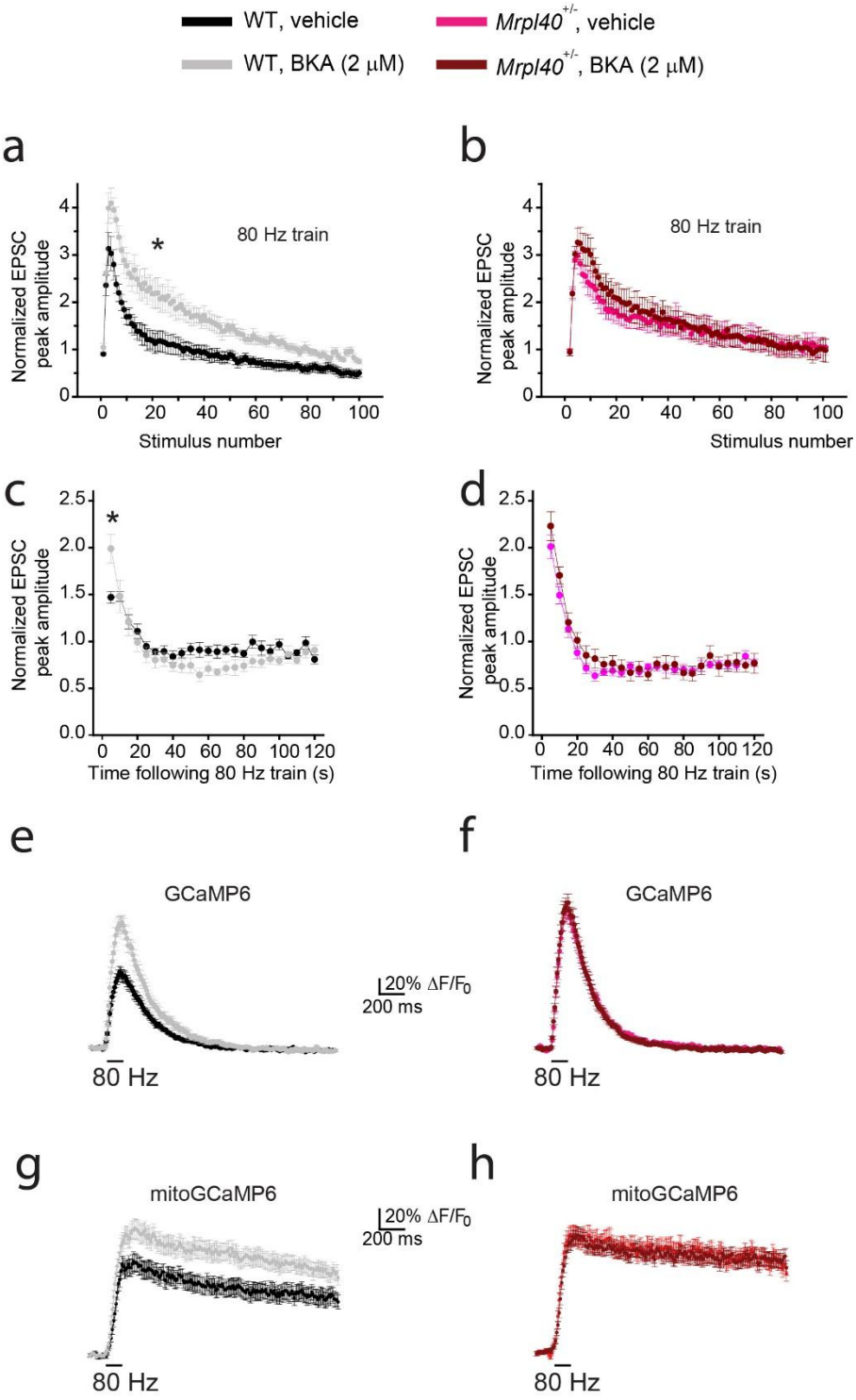

Supplementary Figure 14. The mPTP inhibitor BKA mimics the STP and calcium transient phenotypes of *Mrpl40*$^{+/-}$ mice. (**a-d**) Mean EPSCs during (**a**, **b**) and after (**c**, **d**) the 80-Hz train in WT (**a**, **c**) and *Mrpl40*$^{+/-}$ (**b**, **d**) mice in the absence or presence of BKA. (**e,f**) Average normalized cytosolic GCaMP6 fluorescence intensity as a function of time during the 80-Hz train in WT (**e**) and *Mrpl40*$^{+/-}$ (**f**) mice. (**g, h**) Average normalized mitoGCaMP6 fluorescence intensity as a function of time during the 80-Hz train in WT (**g**) and *Mrpl40*$^{+/-}$ (**h**) mice. **P* <0.05.

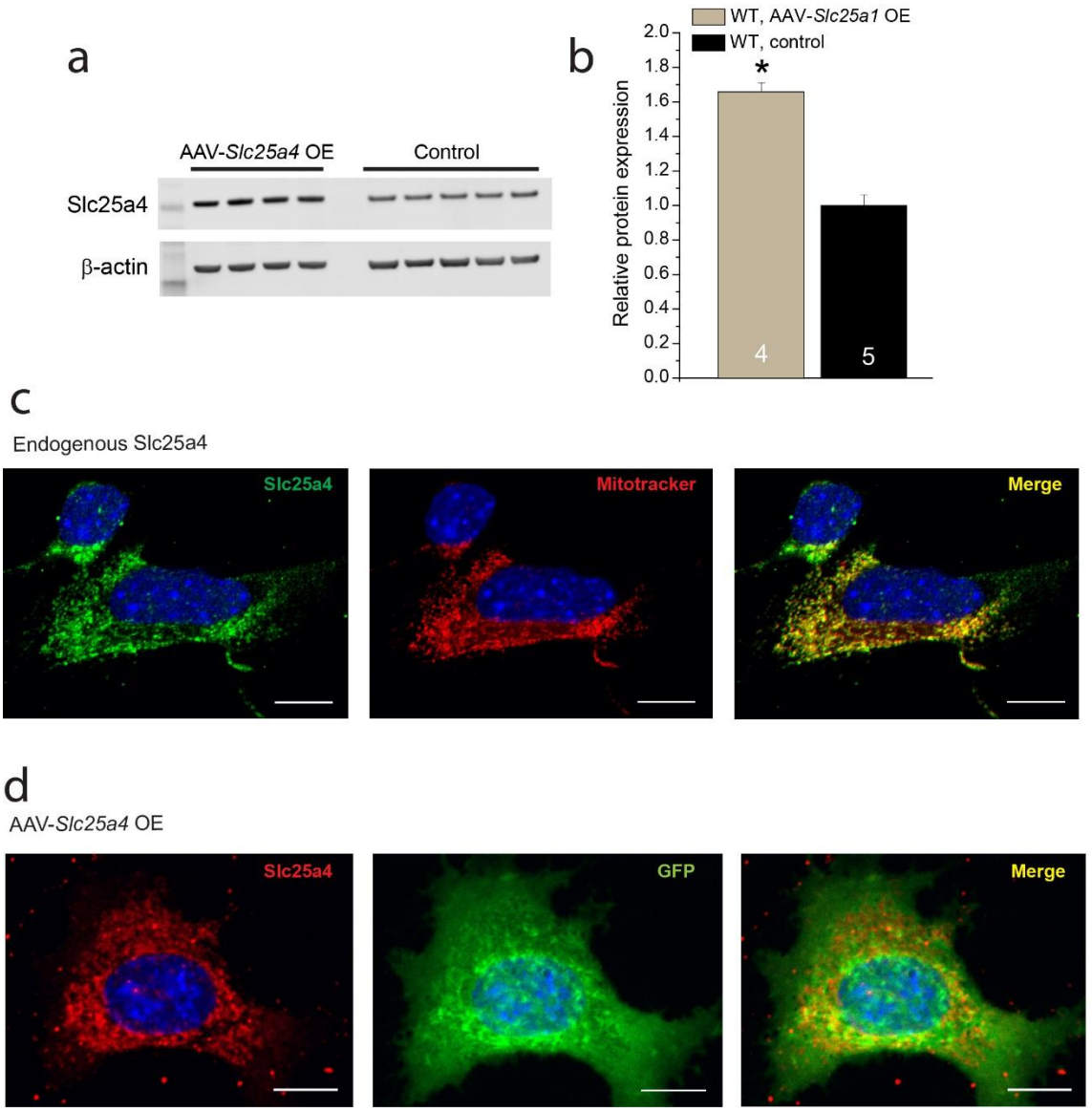

Supplementary Figure 15. Overexpression of *Slc25a4* does not change its localization to mitochondria. (**a**, **b**) Western blotting experiments (**a**) and average Slc25a4 levels (normalized to β-actin) in the hippocampi of mice injected with a control virus or AAV-Slc25a4 OE. Numbers of mice are shown inside columns. **P* <0.05. (**c**) Endogenous Slc25a4 (green) is colocalized with Mitotracker (red), a fluorescent marker of mitochondria, in N2a cells. (**d**) AAV-*Slc25a4* (AAV-*CamKII*α*-GFP-2A-Slc25a4*) does not change the punctate nature of Slc25a4 (red) expression. In contrast, GFP (green) is expressed in the cytosol, and Hoechst stain (blue) indicates nuclei.

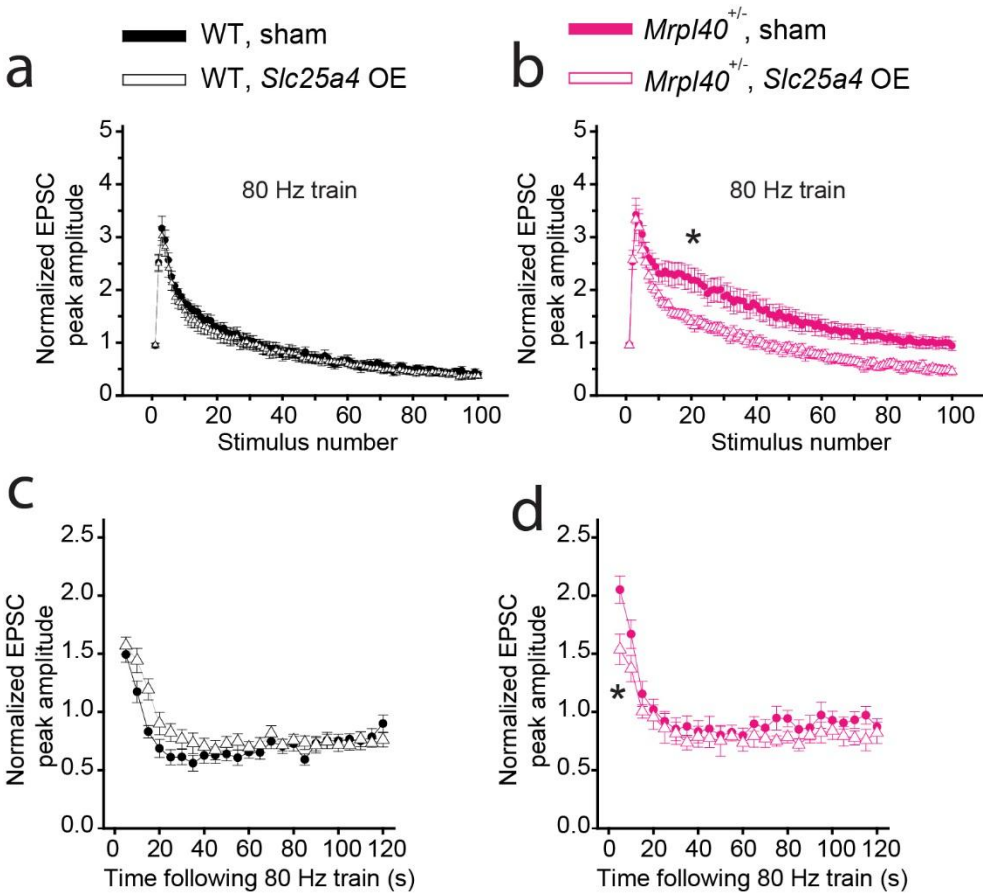

Supplementary Figure 16. *Slc25a4* overexpression rescues the STP phenotypes of *Mrpl40*$^{+/-}$ mice. (**a-d**) STP (**a**, **b**) and augmentation (**c**, **d**) in hippocampal slices from sham- or *Slc25a4*-OE–injected WT and *Mrpl40*$^{+/-}$ mice. **P* <0.05.

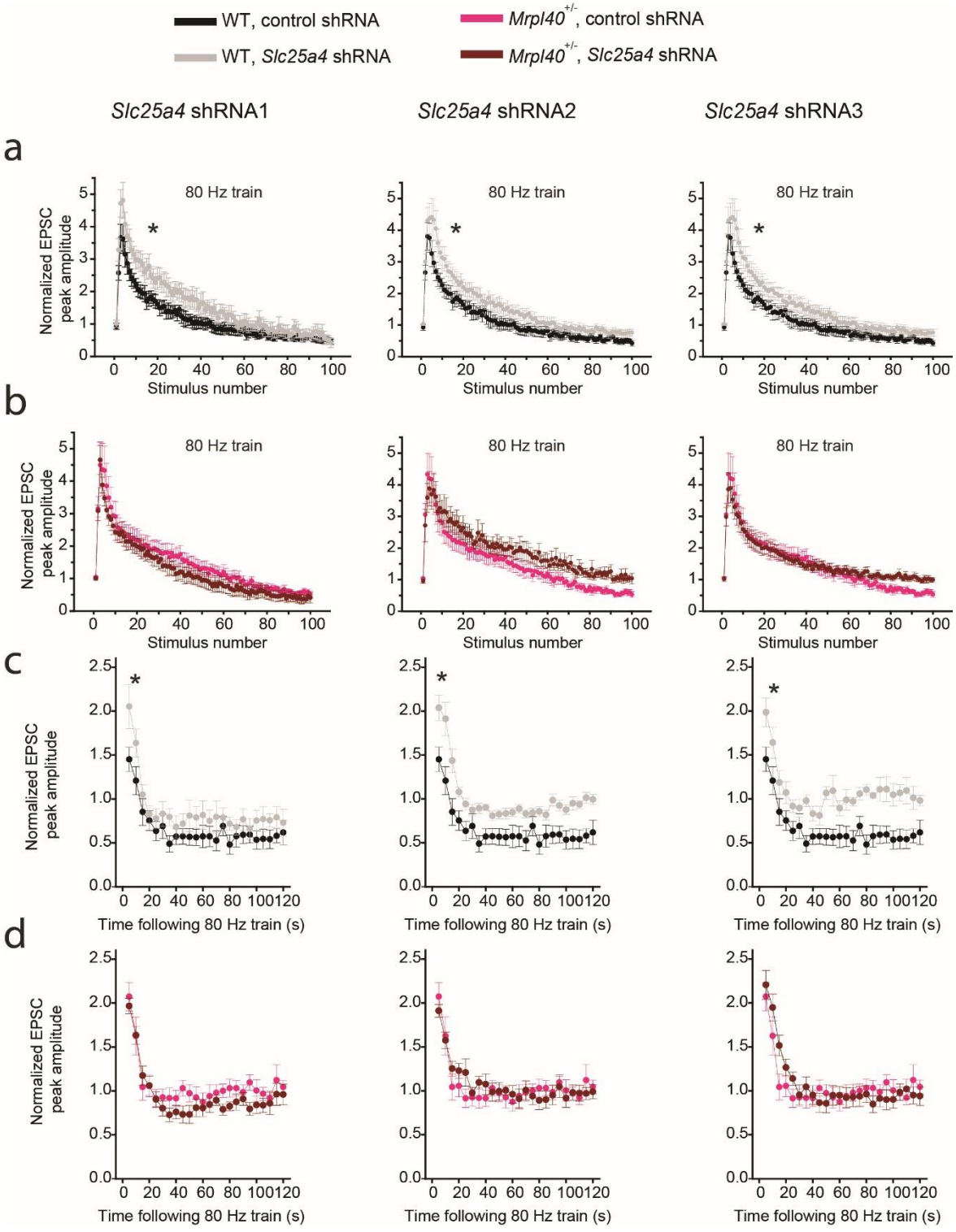

Supplementary Figure 17. *Slc25a4* downregulation mimics the STP phenotypes of *Mrpl40*$^{+/-}$ mice. (**a-d**) STP (**a**, **b**) and augmentation (**c**, **d**) measured in the hippocampal slices from control and *Slc25a4* shRNA–injected WT (**a**,**c**) and *Mrpl40*$^{+/-}$ mice (**b**,d). The data are shown for three different *Slc25a4* shRNAs: shRNA1 (left column), shRNA2 (middle column), shRNA3 (right column).